Supercomputer technologies in inverse problems of ultrasound tomography

Alexander V Goncharsky and Sergey Y Romanov

Research Computing Center, Lomonosov Moscow State University, Moscow, 119991, Russia

E-mail: romanov60@gmail.com

Abstract
The study focuses on the development of efficient methods for solving inverse problems of ultrasound tomography as coefficient inverse problems for the wave equation. The inverse problem consists in finding the unknown wave propagation velocity as a function of coordinates in three-dimensional space. Efficient iterative methods are proposed for solving the inverse problem based on direct computation of the residual functional. One of the most promising directions of ultrasound tomography is the development of ultrasound tomographs for medical research, and primarily for differential diagnosis of breast cancer. From medical viewpoint, diagnostic facilities for differential cancer diagnosis should have a resolution of 3 mm or better. Because of this requirement inverse problems of ultrasound tomography have to be solved on dense grids with sizes of up to 1000x1000 on cross sections of three-dimensional objects studied. Supercomputers are needed to address such inverse problems in terms of the wave model described by second-order hyperbolic equations. The algorithms developed in this study are easily scalable on supercomputers running up to several tens of thousands of processes. The problem of choosing the initial approximation for iterative algorithms when solving the inverse problem has been studied.

PACS
02.30.Zz Inverse problems
02.60.Cb Numerical simulation; solution of equations
02.30.Jr Partial differential equations
02.30.Xx Calculus of variations
43.35.Wa Biological effects of ultrasound, ultrasonic tomography
43.60.Rw Remote sensing methods, acoustic tomography
87.63.dh Ultrasonographic imaging
91.30.Cd Body wave propagation

MSC
15A29 Inverse problems
35R30 Inverse problems (undetermined coefficients, etc.) for PDE
35L05 Wave equation
65K10 Optimization and variational techniques
65C20 Models, numerical methods
65Y05 Parallel computation
68U20 Simulation
92C50 Medical applications (general)

Subjects

Mathematical physics
Computational physics
Medical physics

1. Introduction

Currently, tomographic facilities [1-5] having a number of advantages over X-ray tomography are developed extensively in the USA, Germany, Japan, and Russia. Modern medical science is inconceivable without X-ray tomographic examinations, which have one drawback. Regular use of X-ray tomographs is itself hazardous for patients because of strong radiation exposure. MRT tomographs, along with X-ray tomographs, can produce high-resolution two-dimensional images of scanned areas. MRT tomography has its own limitations, however, it is generally believed to be safer for patients that are subject to repeated examinations. One of the drawbacks of MRT tomography is the high cost of examinations.

The currently developed ultrasound tomographs can be an alternative to X-ray and MRT tomography. The primary task of ultrasound tomography is to address the problems of differential diagnosis of breast cancer – one of the most pressing issues of modern healthcare. From the medical viewpoint, diagnostic facilities for differential cancer diagnosis should have a resolution of 3 mm or better. This requirement makes it necessary to solve inverse problems of ultrasound tomography on dense grids with sizes of up to 1000x1000 or even 2000x2000 on cross sections of three-dimensional objects studied.

From mathematical viewpoint inverse problems arising in ultrasound tomography are much more complex than those of X-ray tomography. The tasks of X-ray tomography can be satisfactorily addressed by linear models of ray optics, where the solution of inverse problems reduces to solving two-dimensional Fredholm equation of the first kind. Modern methods for the solution of linear ill-posed problems allow efficient algorithms to be developed for reconstructing high-resolution two-dimensional tomographic images of three-dimensional objects. Furthermore, these algorithms are easy to implement on a common desktop computer or a notebook.

One of the approaches tries to address inverse problems of ultrasound tomography in terms of linear and nonlinear ray optical models [6-10]. However, this approach cannot provide a description for the physical phenomena associated with the wave nature of the sources and radiation employed, and hence cannot take into account diffraction of ultrasound waves, refraction, rereflection, etc. That is why in this paper we address problems of ultrasound tomography in terms of wave models, which we consider to be most consistent with reality.

Unlike what we have in X-ray tomography, inverse problems of ultrasound tomography involve both transmitted and reflected signals. The sources of ultrasound waves emit pulses of ultrasound energy, which, after crossing the diagnosed object or after reflecting from it, are detected by receivers. Ultrasound tomography can use much greater amounts of data, because the signal detected by each receiver is a function of time rather than just a single number (the total ray absorption determined by the positions of the source and receiver), as is the case in X-ray tomography. Mathematical models of ultrasound tomography can describe such phenomena as diffraction, refraction, rereflection of waves, absorption, etc. Scalar wave approximation, namely, the wave equation -- a hyperbolic partial differential equation of the second kind -- can be used as the simplest model to describe the above physical processes. In this case inverse problems of ultrasound tomography can be viewed as coefficient inverse problems. The latter are nonlinear inverse problems and developing algorithms for their solution is a challenging task.

As a research direction, coefficient inverse problems have been studied extensively since late 20 century [11-14]. From the viewpoint of mathematical methods there are two main approaches to solving inverse problems in terms of wave models. The first approach is based on the use of Green functions. In this case inverse problems of ultrasound tomography can be reduced to a set of nonlinear Fredholm integral equations of the first kind [15]. The resulting problem is ill-posed. Methods of solution of linear and nonlinear inverse problems represented by operator equations are well known and efficient procedures have been developed to solve them [15,16]. This representation is naturally suitable for studying the capabilities of various linear approximations to the nonlinear problem of ultrasound tomography. Such an approximation to the nonlinear problem is evidently valid only in the vicinity of the required solution, and this circumstance restricts rather strongly the potential of linear approximations [17-21].

There is another way to solve inverse problems of ultrasound tomography as coefficient inverse problems for hyperbolic partial differential equations. It was shown in the nonlinear formulation that gradient-based iterative algorithms for the construction of an approximate solution can be built directly by minimizing the residual functional without invoking integral representations involving the Green function. This approach has been called the propagation-backpropagation method [22, 23]. Beilina and

Klibanov [24,25] used this approach to construct the so-called *c-global* methods for solving coefficient inverse problems for hyperbolic-type equations or for the Helmholtz equation. Beilina and Johnson [26], Beilina [27], and Beilina and Clason [28] developed adaptive finite element method for hyperbolic coefficient inverse problems, presented an adaptive algorithm, and the numerical results obtained have demonstrated the efficiency of the proposed algorithms. Goncharskii and Romanov [29] showed that the second approach has a number of advantages from the viewpoint of computer implementation compared to that based on Green's function apparatus [30].

Wiskin et al. [1, 31] obtained a number of interesting results concerning the solution of inverse problems of ultrasound tomography. A distinguishing feature of the proposed approach is that the above authors abandon hyperbolic equation in favor of another approximation, which takes into account only the radiation transmitted through the diagnosed object. This approximation can describe phenomena of diffraction and refraction within a certain range of angles and subject to certain absorption restrictions, however, it is not good at describing the effects of the back reflection of ultrasound wave. The algorithms developed have passed evaluation tests, which involved solving not just model problems. Results of clinical tests obtained on mockup facilities for ultrasound diagnosis of breast cancer have been reported.

Currently, there are no commercially manufactured ultrasound tomographs. The development of ultrasound tomographs has now reached the stage of mock-up studies [1-5]. A number of patents concerning ultrasound tomography have been registered. Most of these patents relate to tomographic schemes where the 3D structure of the object studied is reconstructed from cross sections as a sequence of 2D images [32-34]. There are patents describing reconstruction of the 3D structure directly from the measurements made by receivers located on a certain surface [35-36]. A number of patents describe algorithms for solving the problems of wave diagnostics [37-38].

The large number of publications and patents dedicated to ultrasound tomography is indicative of how much attention to the problems of this field is paid by both mathematicians and medics who are looking forward to new tomographic techniques, first and foremost to those aimed at differential diagnostics of breast cancer. In this paper we try to investigate the limiting capabilities of ultrasound tomographic examinations in terms of a mathematical model based on second-order hyperbolic equation. We propose efficient algorithms for solving inverse problems of ultrasound tomography at a high resolution of up to 1000x1000 or even 2000x2000 on two-dimensional reconstructed cross sections. Iterative algorithms are based on exact computation of the gradient of residual functional, which is determined by solving a certain conjugate problem. We demonstrate the efficiency of the proposed algorithms implemented on a supercomputer by solving a number of model problems.

The specific feature of the ultrasound tomography problems considered is that ultrasound properties of the breast differ little in the cases of healthy and cancerous tissues. The sound speed in water is equal to $c_0 = 1500$ *m/s*, whereas the speed of sound propagation in various breast tissues differs from c_0 by no more than 10% (the speeds of sound propagation in fat and muscular tissue are approximately equal to *1450* and *1570 m/s*, respectively. Different authors report different speeds of sound propagation in a carcinoma. The reported estimates are *1585-1630 m/s* [1], *1530.8 m/s* [39], *1527.4 m/s* [40], *1564 m/s* [41], and *1530/1550 m/s* [42]. Thus the sound speed in a carcinoma differs from $c_0 = 1500$ *m/s* by 10-15% or less.

Hence the speed cross section has to be reconstructed in the case of a very low contrast, when healthy and cancerous tissues differ very little in the speed of sound propagation. This circumstance imposes stringent requirements on the algorithms of the reconstruction of tomographic images.

2. Formulation and methods of solution for the inverse problem

In this paper we study the problem of ultrasound tomography in the framework of two models.

2.1. Base model of wave propagation in non-attenuating media

There are different formulations of coefficient inverse problems for hyperbolic-type equations [22, 24, 43]. In this paper we also address the inverse problem in the scalar approximation. Consider the wave equation that describes some acoustic field $u(r,t)$ in the domain $\Omega \subset R^N$, N=2, 3 bounded by the surface S during time $(0,T)$ with a point source located at r_0

$$c(r)u_{tt}(r,t) - \Delta u(r,t) = \delta(r - r_0) \cdot f(t), \tag{1}$$

$$u(r,t=0) = u_t(r,t=0) = 0, \tag{2}$$

$$\partial_n u\,|_{ST} = p(r,t)\,. \tag{3}$$

Here $c^{-0.5}(r)$ is the wave velocity in the medium; $r \in R^N$, the position of the point in space, and Δ, the Laplacian operator with respect to r. The pulse generated by the source is described by function $f(t)$; $\partial_n u\,|_{ST}$ is the derivative along the normal to the surface S in the domain $S \times (0,T)$, and $p(r,t)$, some known function. We assume that imhomogeneities of the medium are due solely to velocity variations, whereas outside the inhomogeneity domain $c(r) \equiv \text{const}$, where *const* is known.

Wave equation (1) effectively describes such wave effects as diffraction, refraction, and rereflection in non-attenuating media. However, even in the framework of this model the solution of inverse problems of ultrasound tomography requires solving ill-posed problems. The inverse problem consists in finding function $c(r)$ that describes the distribution of inhomogeneities by analyzing experimental measurements of wave $U(s,t)$ at the domain boundary S during time $(0,T)$ for different positions r_0 of the source.

Let us now introduce the following functional of residual

$$\Phi(u(c)) = \frac{1}{2}\|u\,|_{ST} - U\|^2 = \frac{1}{2}\int_0^T \int_S (u(s,t) - U(s,t))^2 \,\mathrm{d}s\,\mathrm{d}t\,. \tag{4}$$

Here $\|\cdot\|^2$ is the squared norm in the $L_2(S \times (0,T))$ space and $U(s,t)$ are the experimental data at the domain boundary S during time $(0,T)$.

The breakthrough results in solving the problems of ultrasound tomography are associated with the computation of the gradient of functional $\Phi(u(c))$. Formulas for the gradient of functional $\Phi(u(c))$ in different formulations were derived by Natterer and Wubbeling [22], Beilina and Klibanov [24], and Goncharskii and Romanov [29].

2.2. Base model of wave propagation in attenuating media

Consider now the problem described by the wave equation in the domain $\Omega \subset R^N$ (N=2,3) bounded by the surface S during time $(0,T)$ with a point source located at point r_0

$$c(r)u_{tt}(r,t) + a(r)u_t(r,t) - \Delta u(r,t) = \delta(r-q)\cdot f(t)\,, \tag{5}$$

$$u(r,t=0) = u_t(r,t=0) = 0\,, \tag{6}$$

$$\partial_n u\,|_{ST} = p(r,t)\,. \tag{7}$$

Here $c^{-0.5}(r)$ is the wave velocity in the medium; $a(r)$ describes attenuation in the medium; $\partial_n u\,|_{ST}$ is the derivative along the normal to the surface S in the domain $S \times (0,T)$, and $p(r,t)$ is a known function. The inverse problem consists in finding functions $c(r)$ and $a(r)$ that describe the inhomogeneities given measurements of wave $U(s,t)$ at the domain boundary S during time $(0,T)$ for different source positions r_0. Natterer [44] considered the coefficient inverse problem for hyperbolic-type equations with attenuation in a different formulation.

Problem (5-7) is known to define $u(c,a)$ as an implicit function of $c(r)$ and $a(r)$. Let us now formulate the inverse problem as that of minimizing the following quadratic functional

$$\Phi(u(c,a)) = \frac{1}{2}\|u\,|_{ST} - U\|^2 = \frac{1}{2}\int_0^T \int_S (u(s,t) - U(s,t))^2 \,\mathrm{d}s\,\mathrm{d}t\,. \tag{8}$$

with respect to functions $c(r)$ and $a(r)$. Here $\|\cdot\|^2$ is the squared norm in the $L_2(S \times (0,T))$ space and $U(s,t)$ are the experimental wave measurements at the domain boundary S during time $(0,T)$.

The inverse problems considered are ill posed, and therefore regularization terms can be added to functionals (4) and (8). However, we can do without such terms in these functionals, because the iterative methods used to solve the corresponding problems have, in a sense, certain regularizing properties [15]. We now write out the formulas for the gradients of residual functionals (4) and (8). Let us formulate the

mathematical problem that will allow us to compute the gradient of functional (8). We denote by ξ the pair $\xi = (c, a)$, $u_\xi \mathrm{d}\xi = u_c \mathrm{d}c + u_a \mathrm{d}a$ and find the component of the increment of functional (8) that is linear in arbitrary variation $\mathrm{d}\xi = (\mathrm{d}c, \mathrm{d}a)$

$$\mathrm{d}\Phi'(u(\xi)) = \int_{ST} (u - U)(u_\xi \mathrm{d}\xi)\mathrm{d}s\,\mathrm{d}t\,, \tag{9}$$

where u_ξ is the Frechet derivative.

Function $u(r,t)$ is a solution of problem (5-7) for some $\xi(r)$ (i.e., $u(r,t)$ is an implicit function of $\xi(r)$) and hence taking the total derivative with respect to $\xi(r)$ in formula (5) yields

$$\begin{cases} c(r)(u_c \mathrm{d}c)_{tt} + a(r)(u_c \mathrm{d}c)_t - \Delta(u_c \mathrm{d}c) + u_{tt}(r,t)\mathrm{d}c = 0 \\ c(r)(u_a \mathrm{d}a)_{tt} + a(r)(u_a \mathrm{d}a)_t - \Delta(u_a \mathrm{d}a) + u_t(r,t)\mathrm{d}a = 0 \end{cases}. \tag{10}$$

We then introduce linear operator P that consists in constraining function to the domain $t = 0$ and find from equation (6) that $u(r,t=0) \equiv P(u(r,t)) = 0 = \mathrm{const}$. We now differentiate this relation with respect to $\xi(r)$ to obtain $(P(u(r,t)))_\xi d\xi = P(u_\xi \mathrm{d}\xi) = (u_\xi \mathrm{d}\xi)(r,t=0) = 0$. It similarly follows from equations (6) and (7) that

$$(u_\xi \mathrm{d}\xi)(r,t=0) = (u_\xi \mathrm{d}\xi)_t(r,t=0) = 0\,, \tag{11}$$

$$\partial_n (u_\xi \mathrm{d}\xi)|_{ST} = 0\,. \tag{12}$$

Function $(u_\xi \mathrm{d}\xi)(r,t)$ is thus a solution of problem (10-12) for any variation $\mathrm{d}\xi = (\mathrm{d}c, \mathrm{d}a)$. We now introduce operator A: $Au = c(r)u_{tt}(r,t) + a(r)u_t(r,t) - \Delta u(r,t)$.

Consider what we call the "conjugate" problem to the main problem (5-7)

$$Bw = c(r)w_{tt}(r,t) - a(r)w_t(r,t) - \Delta w(r,t) = 0\,, \tag{13}$$

$$w(r,t=T) = w_t(r,t=T) = 0\,, \tag{14}$$

$$\partial_n w|_{ST} = u|_{ST} - U\,, \tag{15}$$

where u is the solution of the main problem (5-7). Let us denote $(u_\xi \mathrm{d}\xi)(r,t) = \tilde{u}(r,t)$ for some variation $\mathrm{d}\xi$. Consider now the scalar product $(Bw, \tilde{u})$. We use equations (11), (14), and (15) to obtain

$$\begin{aligned} 0 = (Bw, \tilde{u}) &= \int_{\Omega T} (Bw)\tilde{u}\,\mathrm{d}r\,\mathrm{d}t \\ &= \int_{\Omega 0}^{T} c(r)w_{tt}(r,t)\tilde{u}(r,t)\mathrm{d}t\,\mathrm{d}r - \int_{\Omega 0}^{T} a(r)w_t(r,t)\tilde{u}(r,t)\mathrm{d}t\,\mathrm{d}r - \int_{0\Omega}^{T} \Delta w(r,t)\tilde{u}(r,t)\mathrm{d}r\,\mathrm{d}t \\ &= -\int_{\Omega 0}^{T} c(r)w_t(r,t)\tilde{u}_t(r,t)\mathrm{d}t\,\mathrm{d}r + \int_{\Omega 0}^{T} a(r)w(r,t)\tilde{u}_t(r,t)\mathrm{d}t\,\mathrm{d}r - \int_{0S}^{T} \partial_n w(s,t)\tilde{u}(s,t)\mathrm{d}s\,\mathrm{d}t \\ &+ \int_{0\Omega}^{T} \nabla w(r,t)\nabla\tilde{u}(r,t)\mathrm{d}r\,\mathrm{d}t = -\int_{\Omega 0}^{T} c(r)w_t(r,t)\tilde{u}_t(r,t)\mathrm{d}t\,\mathrm{d}r + \int_{\Omega 0}^{T} a(r)w(r,t)\tilde{u}_t(r,t)\mathrm{d}t\,\mathrm{d}r \\ &- \int_{ST} (u(s,t) - U(s,t))\tilde{u}(s,t)\mathrm{d}s\,\mathrm{d}t + \int_{0\Omega}^{T} \nabla w(r,t)\nabla\tilde{u}(r,t)\mathrm{d}r\,\mathrm{d}t\,. \end{aligned}$$

We thus have

$$\int_{ST} (u(s,t) - U(s,t))\tilde{u}(s,t)\mathrm{d}s\,\mathrm{d}t =$$

$$= -\int_{\Omega}\int_{0}^{T} c(r) w_t(r,t) \tilde{u}_t(r,t)\,\mathrm{d}t\,\mathrm{d}r + \int_{\Omega}\int_{0}^{T} a(r) w(r,t) \tilde{u}_t(r,t)\,\mathrm{d}t\,\mathrm{d}r + \int_{0}^{T}\int_{\Omega} \nabla w(r,t) \nabla \tilde{u}(r,t)\,\mathrm{d}r\,\mathrm{d}t \,. \quad (16)$$

We then consider the scalar product $\langle w, A\tilde{u} \rangle$ and use equations (6), (10), and (14) to obtain

$$\langle w, A\tilde{u} \rangle = \int_{\Omega T} w(r,t) A(\tilde{u}(r,t))\,\mathrm{d}r\,\mathrm{d}t$$

$$= -\int_{\Omega}\int_{0}^{T} \left[w(r,t) u_{tt}(r,t)\,\mathrm{d}c(r) + w(r,t) u_t(r,t)\,\mathrm{d}a(r) \right] \mathrm{d}t\,\mathrm{d}r$$

$$= \int_{\Omega}\int_{0}^{T} \left[w_t(r,t) u_t(r,t)\,\mathrm{d}c(r) + w_t(r,t) u(r,t)\,\mathrm{d}a(r) \right] \mathrm{d}t\,\mathrm{d}r \,. \quad (17)$$

On the other hand, we use equations (11), (12), and (14) to obtain

$$(w, A\tilde{u}) = \int_{\Omega}\int_{0}^{T} w(r,t) c(r) \tilde{u}_{tt}(r,t)\,\mathrm{d}t\,\mathrm{d}r + \int_{\Omega}\int_{0}^{T} w(r,t) a(r) \tilde{u}_t(r,t)\,\mathrm{d}t\,\mathrm{d}r - \int_{0}^{T}\int_{\Omega} w(r,t) \Delta \tilde{u}(r,t)\,\mathrm{d}r\,\mathrm{d}t$$

$$= -\int_{\Omega}\int_{0}^{T} c(r) w_t(r,t) \tilde{u}_t(r,t)\,\mathrm{d}t\,\mathrm{d}r + \int_{\Omega}\int_{0}^{T} a(r) w(r,t) \tilde{u}_t(r,t)\,\mathrm{d}t\,\mathrm{d}r$$

$$= \int_{0}^{T}\int_{S} w(s,t) \partial_n \tilde{u}(s,t)\,\mathrm{d}s\,\mathrm{d}t + \int_{0}^{T}\int_{\Omega} \nabla w(r,t) \nabla \tilde{u}(r,t)\,\mathrm{d}r\,\mathrm{d}t$$

$$= -\int_{\Omega}\int_{0}^{T} c(r) w_t(r,t) \tilde{u}_t(r,t)\,\mathrm{d}t\,\mathrm{d}r + \int_{\Omega}\int_{0}^{T} a(r) w(r,t) \tilde{u}_t(r,t)\,\mathrm{d}t\,\mathrm{d}r + \int_{0}^{T}\int_{\Omega} \nabla w(r,t) \nabla \tilde{u}(r,t)\,\mathrm{d}r\,\mathrm{d}t \,. \quad (18)$$

We derive from equations (17) and (18)

$$\int_{\Omega}\int_{0}^{T} \left[w_t(r,t) u_t(r,t)\,\mathrm{d}c(r) + w_t(r,t) u(r,t)\,\mathrm{d}a(r) \right] \mathrm{d}t\,\mathrm{d}r$$

$$= -\int_{\Omega}\int_{0}^{T} c(r) w_t(r,t) \tilde{u}_t(r,t)\,\mathrm{d}t\,\mathrm{d}r + \int_{\Omega}\int_{0}^{T} a(r) w(r,t) \tilde{u}_t(r,t)\,\mathrm{d}t\,\mathrm{d}r + \int_{0}^{T}\int_{\Omega} \nabla w(r,t) \nabla \tilde{u}(r,t)\,\mathrm{d}r\,\mathrm{d}t \,. \quad (19)$$

It then follows from equations (9), (16), and (19) that

$$\mathrm{d}\Phi'(u(\xi)) = \int_{ST} \langle -U, u_\xi \rangle\,\mathrm{d}\xi\,\mathrm{d}s\,\mathrm{d}t = \int_{\Omega} \left[w_t(r,t) u_t(r,t)\,\mathrm{d}c(r) + w_t(r,t) u(r,t)\,\mathrm{d}a(r) \right] \mathrm{d}t\,\mathrm{d}r$$

$$= \int_{\Omega} \left\{ \left[\int_{0}^{T} w_t(r,t) u_t(r,t)\,\mathrm{d}t \right] \mathrm{d}c(r) + \left[\int_{0}^{T} w_t(r,t) u_t(r,t)\,\mathrm{d}t \right] \mathrm{d}a(r) \right\} \mathrm{d}r \,.$$

We now isolate the terms that are linear in variations $\mathrm{d}c$ and $\mathrm{d}a$ to derive the following final formula for the gradient of functional $\Phi(u(\xi))$

$$\begin{cases} \Phi'_c\ (u(c)) = \int_{0}^{T} w_t(r,t) u_t(r,t)\,\mathrm{d}t \\ \Phi'_a\ (u(a)) = \int_{0}^{T} w_t(r,t) u(r,t)\,\mathrm{d}t \end{cases} . \quad (20)$$

Here $u(r,t)$ is the solution of the main problem (5-7) and $w(r,t)$, that of the "conjugated" problem (13-15) for the given $c(r)$ and $a(r)$. Hence to compute the gradient of the functional, we have to solve both the main and "conjugate" problems.

We now set $a(r)$ =0 to derive the following formula for the gradient of functional (4) for non-attenuating media

$$\Phi_c'(u(c)) = \int_0^T w_t(r,t)u_t(r,t)\,\mathrm{d}t\,. \qquad (21)$$

Here $u(r,t)$ is the solution of the main problem (1-3) and $w(r,t)$, that of the following "conjugate" problem (22-24) for the given $c(r)$

$$c(r)w_{tt}(r,t) - \Delta w(r,t) = 0\,, \qquad (22)$$

$$w(r,t=T) = w_t(r,t=T) = 0\,, \qquad (23)$$

$$\partial_n w|_{ST} = u|_{ST} - U\,, \qquad (24)$$

where *u* is the solution of the main problem (1-3). Thus to compute the gradient of the functional, it is necessary to solve both the main and the "conjugate" problems.

Given Φ_c' from equation (21), one can build various iterative schemes for minimizing the functional of residual (4). The numerical methods employed in this paper use the steepest descent method to numerically solve at each iteration the problem of one-dimensional minimum search in the gradient direction. Other gradient methods including regularized iterative procedures [15] can also be used to this end.

Similarly, for model (5-7) iterative procedures can be built to determine functions *c(r)* and *a(r)* using formula (20) for the gradient of the residual functional of the problem with attenuation. Numerical methods are the same for basic models of wave propagation in both media with and without attenuation. We therefore performed model computations for the basic model without attenuation in order to investigate the limiting capabilities of the algorithms of the reconstruction of the speed cross section in problems of ultrasound tomography. This is the most popular model in all studies involving inverse problems of wave tomography [12, 13, 14, 18, 19, 22, 24]. Another aim of modeling is to find out what is the effect of diffraction, refraction, and rereflection on the reconstruction of images.

3. Numerical algorithms for solving the inverse problem

Solving inverse problems of ultrasound tomography in the above formulation of equation (1) in three-dimensional space R^3 is a difficult task. The formula for the gradient of functional $\Phi(u(c))$ can be used to compute Φ_c' in the case $c(r)$ $r \in R^3$ if receivers are located on a two-dimensional surface *S*. In this formulation the inverse problem of ultrasound tomography appears to be rather difficult to implement even on modern supercomputers.

In this paper we follow the traditional tomographic approach and consider the problem of reconstructing a three-dimensional object as a set of two-dimensional problems of reconstructing the object cross sections. We further assume that the propagation of ultrasound wave in each of the cross sections can be described by equation (1) in the R^2 space at fixed *z*, so that $r=(x,y)$. We use formula (21) where $r \in R^2$ to compute the gradient of the functional of residual**.** We similarly compute the functional of residual $\Phi(u(c))$ by function $u(r,t)$, where $r \in R^2$ **.**

We use the finite difference method to solve the inverse problem on each of the two-dimensional cross sections. In this formulation solving differential wave equations reduces to solving difference equations. We introduce the following uniform grid in the domain of function arguments

$$v_{ijk} = (x_i, y_j, t_k) : x_i = ih, 0 \le i < n; y_j = jh, 0 \le j < n; t_k = k\tau, 0 \le k < m\,,$$

where *h* and τ are the grid size in the spatial and time directions, respectively. Parameters *h* and τ are related by the Courant stability condition $c^{-0.5}\tau < h$, where $c^{-0.5}(r)$ is the wave velocity.

We use the following approximations to the second-order derivatives in equation (1)

$$u_{tt}(r,t) = \frac{u_{ijk+1} - 2u_{ijk} + u_{ijk-1}}{\tau^2},$$

$$\Delta u(r,t) = \frac{u_{i+1jk} - 2u_{ijk} + u_{i-1jk}}{h^2} + \frac{u_{ij+1k} - 2u_{ijk} + u_{ij-1k}}{h^2}.$$

In a source-free domain we obtain the following explicit difference scheme for differential equation (1)

$$c_{ij}\frac{u_{ijk+1} - 2u_{ijk} + u_{ijk-1}}{\tau^2} - \frac{u_{i+1jk} - 2u_{ijk} + u_{i-1jk}}{h^2} - \frac{u_{ij+1k} - 2u_{ijk} + u_{ij-1k}}{h^2} = 0. \quad (25)$$

Here u_{ijk} is equal to the value of function $u(r,t)$ at point (x_i, y_j) at time t_k, and c_{ij} is equal to the value of function $c(r)$ at point (x_i, y_j).). In the model computations reported in this paper we use perfectly absorbing boundary conditions [45].

$$\partial_n u|_{ST} = -c^{0.5}\partial_t u|_{ST}.$$

In model computations the domain studied is surrounded by a uniform medium, where the process of propagation of the sounding pulse is well understood, allowing $u(r,t)$ and $u_t(r,t)$ to be computed for small t. We give the form of the sounding pulse in Section 5.

The difference scheme for *w* can be written in a similar way. The solution can be found explicitly by time layers. Gradient (21) of functional (4) can be computed by the following difference formula

$$grad_{ij} = \sum_{k=0}^{m} \frac{u_{ijk+1} - u_{ijk}}{\tau} \frac{w_{ijk+1} - w_{ijk}}{\tau} \tau. \quad (26)$$

We now describe the steepest descent algorithm for the numerical solution of inverse problem. The iterative sequence $c^{(n)}$ for minimizing residual functional (4) is built as follows.

(1) We start with the initial approximation $c^{(0)} = c_0 = const$.

(2) For $c^{(0)}$ we solve direct problem (1-3) in the difference approximation. We then use explicit difference scheme (25) to solve the direct problem of computing $u(r,t)$ at each detector.

(3) We then solve conjugate problem (22-24) in the difference approximation for function $u(r,t)$ obtained for each detector. As a result, we obtain $w(r,t)$ at each grid point.

(4) We use the resulting $u(r,t)$ and $w(r,t)$ values to compute gradient $\Phi_c'(u(c^{(0)}))$ (21) of the functional by formula (26).

(5) We then use the inferred gradient at point $c^{(0)}$ to find the minimum of functional $\Phi(c^{(0)} - \gamma\Phi_c'(c^{(0)}))$ with respect to parameter γ in the domain $\gamma > 0$.

(6) We set $c^{(1)}$ equal to the point of minimum of the functional and the process returns to stage (1).

4. Use of supercomputer technologies for implementing numerical methods for solving inverse problems of ultrasound tomography

Modern supercomputers are capable of performing computations simultaneously on several tens and even seven hundred thousand processors. Superscalability is the capability of the development process that allows the resulting algorithms to be run on arbitrarily large number of processors so that the computing time decreases with the number of processors. The procedures devised in this paper proved to be suitable for supercomputers and allowed highly efficient superscalable numerical algorithms to be developed.

The efficiency of parallel computations in solving the inverse problem is determined by the structure of the algorithm and its decouplability into a large number of computationally independent units.

The problem of the diagnostic of a 3D object is considered as a set of two-dimensional problems each of which is a coefficient inverse problem for a hyperbolic-type equation. Joint analysis of cross sections is used to describe the three-dimensional structure of the object. In this approach computations in each cross section are performed independently. The computations for both direct and conjugate problem

for each source position can also be performed independently. Hence parallelizing computations by decoupling them into cross sections and sources is most efficient.

Explicit schemes prove to be efficient from the viewpoint of algorithm parallelization. In such schemes the computation of the function value at point (x_i, y_j, t_k) at the new layer depends only on the nearest points on the current and previous layers. The proposed method of spatial parallelization consists in subdividing the common field into equal portions with computations for each such portion performed by a different computing core. To compute the function values at a point located at the boundary of a portion, the function values at the corresponding boundary of the neighbouring portion at the previous time layer must be known. We therefore add on each side of the portion a row or column containing the values from the corresponding boundary of the neighbouring portion. In this way each process performs computations for the new time layer in the inner region of its allocated portion of the common field independently of the other processes and then exchanges the boundary values with its "neighbours". Such organization allows highly scalable numerical methods to be developed for solving the coefficient inverse problem.

Table 1 lists the results of numerical benchmarking of the methods developed for the ultrasound tomography problem considered here. Test computations were run on the supercomputer of the Supercomputing Center of Lomonosov Moscow State University [46]. We give the computing times for 15 iterations of the iterative process for a single cross section and a single source for different partitionings of the cross section into square subregions (one CPU core per subregion with the number of cores varying from 1 to 100). As is evident from Table 1, increasing the number of cores to 100 decreases the computing time for the inverse problem on one cross section by a factor of 45. The data listed in Table 1 demonstrate that the proposed algorithms are scalable, i.e. the computing time decreases with increasing number of processors. Correspondingly, the solution of the a problem with 8 sources on 40 cross sections is effectively parallelized on 32000 CPU cores resulting in a factor of 14000 advantage compared computations using a single processor.

Table 1. Results of testing on "Lomonosov" supercomputer.

Number of processes	1	4	9	16	25	36	49	64	81	100
Computing time for 15 iterations (T), (s)	1893	903	370	291	162	121	67	64	44	40

Although the above results demonstrate high efficiency of supercomputers in solving the problem in question, we do not consider the algorithms developed to be optimal from computational viewpoint. Optimization of algorithms is obviously a task of great importance, which can be addressed using various methods, e.g., finite-element methods, implicit difference schemes, and other minimization techniques such as the conjugate gradient method etc. Note that the problem of optimizing algorithms on supercomputers has certain specific features. Simple algorithms, e.g. those based on explicit difference schemes, often prove to work better than implicit schemes, which are usually more efficient when run on single-processor systems. The possibility of parallelizing computations into the maximum number of individual processes with small amount of data exchange is an important property characterizing algorithms used on supercomputers. In this case the computing time decreases with increasing number of computing cores, i.e., the program is scalable. In this study we developed superscalable software involving several tens of thousands of processes.

5. Model computations

We developed efficient methods for solving the inverse problem of ultrasound tomography based on explicit computation of the gradient of the residual functional. We developed a supercomputer software kit, which can be used to solve many problems involving optimization of the parameters of ultrasound tomographs at the design stage. We investigated how the quality of reconstruction depends on the number of sources and receivers, discretisation levels, pulse shape, wavelength, number of grid points, the distance from transducers to the object, etc. The paper size restrictions limits the number of illustrations - we show only a small part of them.

We used the mathematical model described by equation (1). Figure 1 shows the experimental design: the numbers 1 and 2 indicate the sources and receivers, respectively. Eight sources are located at the midpoints of the sides and at the corners of the square and receivers are placed along the perimeter of the computational domain. The region studied (G) is located at the centre of the square and surrounded by medium L with known wave propagation velocity c_0.

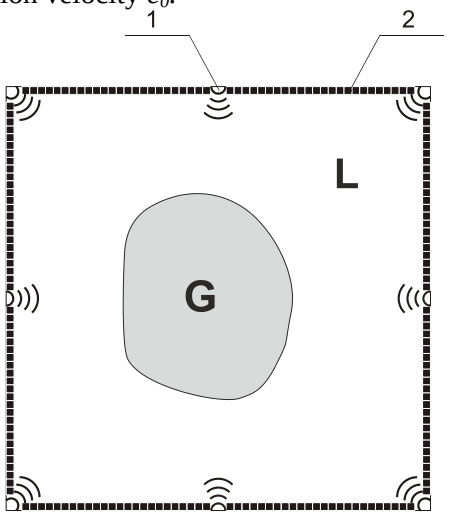

Figure 1. Experimental design: the region studied (G) and domain L with known wave propagation velocity c_0.

We consider a sounding pulse at some time $t_1 > 0$ in the form of a spherically propagating wave in medium L given by the formula

$$\begin{cases} u(r,t_1) = \exp(\alpha(r\text{-}R_0))\sin\left(\dfrac{4\pi(r\text{-}R_0)}{c_0 T}\right), \quad \text{at} \quad R_0 - c_0 T < r < R_0 \\ u(r) = 0, \quad \text{in other cases} \end{cases}, \tag{27}$$

where r is the distance from the current point to the pulse source; T, the pulse duration; c_0, the wave propagation velocity in medium L ; R_0, the distance from the leading edge of the wave to the pulse source, and $\alpha > 0$, a parameter.

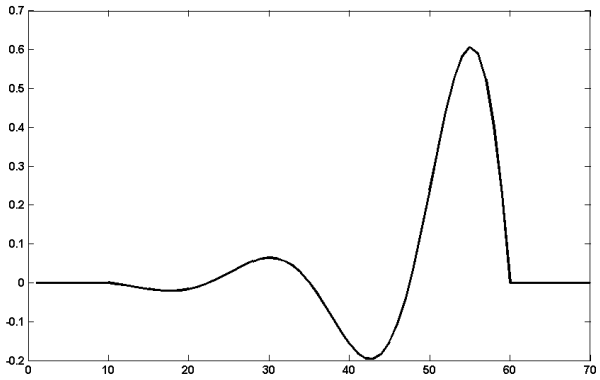

Figure 2. Plot of sounding pulse

Figure 2 shows the plot of sounding pulse with the following parameters: $\alpha = 0.45$, R_0=10 mm, c_0=1500000 mm/s, and T=0.00000666 s.

Function $u(r,t_1)$ has a compact support equal to about two wavelengths. Real signal sours are characterized by different signals $u(r,t_1)$. The form of the signal depends on the material the sources are made of, their structure, and the electric signal applied to them. Within the framework of certain models

the electric signal can be computed to be generated and fed to a source in order to obtain the required initial pulse $u(r,t_1)$. A characteristic feature of all pulses $u(r,t_1)$ is a certain number of oscillations as shown in Fig. 2. The smaller are these oscillations, the better. In the idealized case there should be no oscillations. Development of sources and receivers for ultrasound tomography constitute a special field of research [3].

The use a supercomputer made it possible to perform an extensive numerical analysis of the solution of the inverse problem over a wide range of parameters. The main parameters of the problem varied in the following intervals:

1) sound wavelength – from 5 to 10 mm;
2) vertical and horizontal size of the ultrasonography region – from 15 to 20 cm;
3) number of grid points along the horizontal coordinates from 500x500 to 2000x2000;
4) number of vertical data recording cross sections – up to 40;
5) number of sources – from 4 to 32;
6) distance between receivers in wavelengths – from λ/4 to 3λ, where λ is the wavelength.
7) input data error level 0% to 15%.

We solved more than 100 two-dimensional model reconstructions of the speed cross section with different parameters. We solved model problems both with extra errors added to experimental data and with exact data. As an example, we present the results of the computation for different number of sources. Figure 3 shows the results of the computation of the model problem solved without introducing extra errors. The exact solution of the problem coincides with that shown in Fig. 4a. The wavelength is λ = 5 mm. The minimum size of irregularities was about 2 mm and the size of the irregularity domain was on the order of 15 cm.

Figures 3a-c show the results of the reconstruction of the speed function obtained using eight sources and 10, 170, and 500 iterations, respectively. Figure 3d shows the speed cross section obtained using four wave sources and 500 iterations. The interreceiver distance was equal to ~ λ/2. As is evident from Figs 3. a-c, the approximate solution obtained with the first 10 iterations is very far from the exact solution. The approximate solution obtained at the 170th iteration reproduces the shape of the irregularity. One can easily see artefacts both inside the region studied and outside it. However, this figure demonstrates sufficiently good resolution even for small objects with sizes of 2mm. The solution obtained at the 500th iteration reproduces well not only the shape of the irregularity and the absolute speed value. Artefacts are practically absent. Figure 3d shows the reconstructed cross section for the same problem, but obtained with four sources. A comparison of the results obtained at the 500th iteration shows that artefacts are present in the solution obtained with four sources and absent in the solution obtained with eight sources.

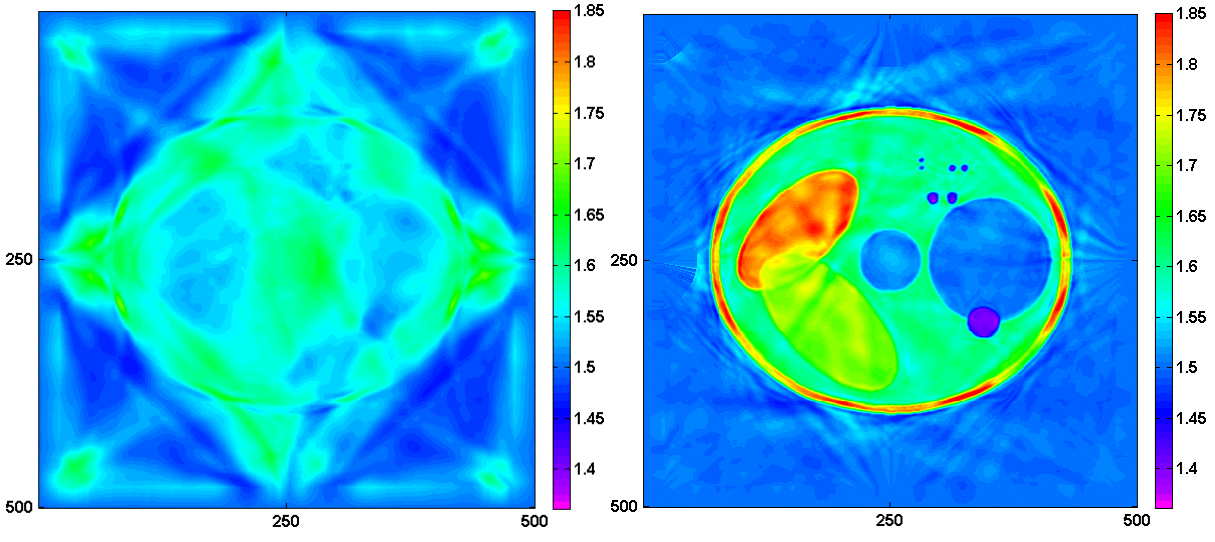

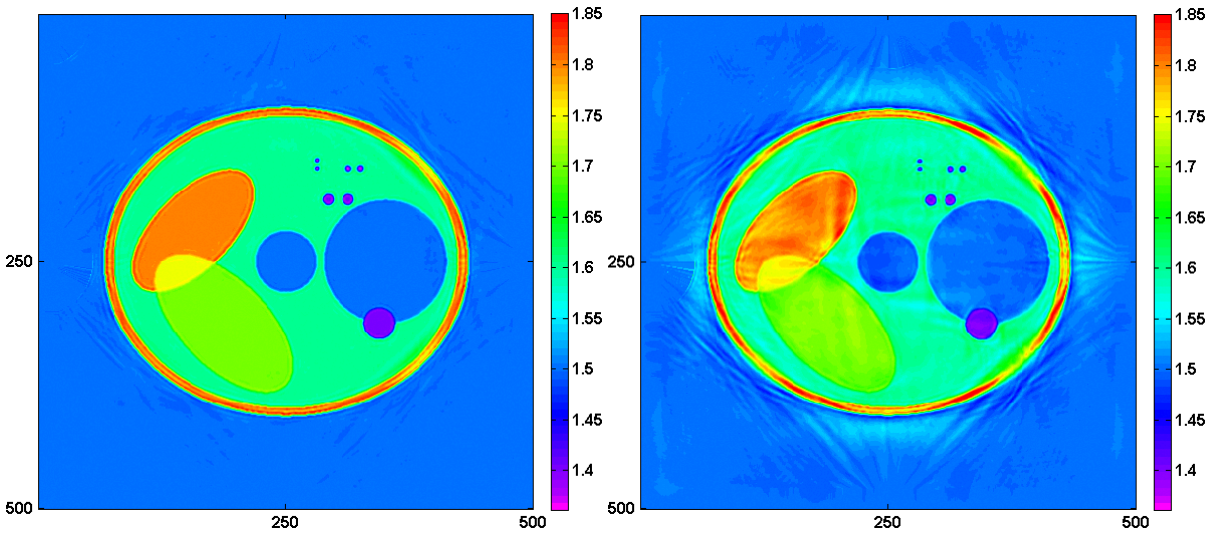

Figure 3 (a - d). Results of model computations: (a) 10 iterations, eight sources; (b) 170 iterations, eight sources; (c) 500 iterations, eight sources; (d) 500 iterations, four sources.

Table 2 lists the values of the residual functional for 10, 170, and 500 iterations and four and eight sources, respectively. As is evident from the Table, the functional of residual for 500 iterations and four sources is 10 times greater than the value of the functional of residual for eight sources.

Table 2. Values of the functional of residual.

Number of iterations	10	170	500
Functional of residual;, four sources	$4.91 \cdot 10^{-4}$	$2.37 \cdot 10^{-5}$	$1.26 \cdot 10^{-6}$
Functional of residual;, eight sources	$3.66 \cdot 10^{-4}$	$4.19 \cdot 10^{-6}$	$1.26 \cdot 10^{-7}$
Computing time (min)	0.5	7	20

We performed model computations on a 500x500 grid. Such a number of grid points ensures sufficiently small approximation error to solve problems with several percent errors in experimental data. The computing time listed in Table 2 was obtained when running the program on 64 CPU cores.

The aim of obtaining the results presented below was to achieve the best possible performance in ultrasound tomography, and they correspond to smaller errors and smaller functional values. We performed such studies to analyze the effect of diffraction, determine the performance limits of tomographic facilities in terms or resolution etc. In this case we performed our model computations on a 1000x1000 grid.

One of the purposes of our numerical simulations was to study the capabilities of the supercomputer for simultaneous computation of a large number of cross sections, which is a real task to be performed on ultrasound tomographic facilities [3, 4]. To this end, we carried out experimental studies on a computer-synthesized 3D object with model irregularities with sizes up to 150 mm. The minimal size of irregularity was 2 mm. The z coordinate distance between cross sections in this model problem is a conventional parameter, because in the model experiment the data in each cross section were computed in two-dimensional space and therefore the parameter in question affects only the number of reconstructed cross sections. Strictly speaking, it would be more correct to use three-dimensional numerical algorithms for computing the direct problem on detectors located on planes parallel to the *x*,*y* plane.

Variation of velocity $c(x, y, z)$ in the model problem did not exceed 10%. We performed model computations for 5 mm wavelengths and eight sources. The interreceiver distance was 2.4 mm; the horizontal and vertical size of the ultrasound sounding domain was equal to 200x200 mm^2 and 200 mm, respectively. The computations were performed on a 1002x1002 grid. All computations started with the initial approximation $c_0 = const$. In our model computations we set the distance between cross sections equal to 5 mm.

It would be good for real facilities to have the same resolution of 2--3 mm or less in all three coordinates x, y, and z. Unlike what we have in the case of x-ray tomography, the possibility to reduce the pixel size in z in ultrasound tomography is limited by the requirement that cross sections in z should be independent of each other. The cross-section thickness that allows them to be considered as independent is determined not by computational schemes, but primarily by the effects of diffraction, refraction, rereflection, etc. For a more detailed discussion of the possibility for ultrasound tomography to reconstruct independent cross sections that are 2--3 mm apart see Section 6 of this paper.

In our simulations of the reconstruction of 3D irregularity we solved the direct problem of ultrasound wave propagation in each two-dimensional domain without introducing extra simulated errors. We then used the data obtained to solve the inverse problem of reconstructing function $c(x, y, z)$ at each fixed $z = z_i$ ($i = 1, \ldots 40$). Because of the paper size restrictions we show in Figs. 4--7 only the results of reconstruction for each 10th cross section of the the speed of ultrasound wave propagation in the object studied as a function of x, y at fixed $z = z_i$ ($i = 1, \ldots 40$).

The left-hand panels of Figs. 4--7 show the cross sections of the phantom. The right-hand panels show the resulting reconstructed images. Speed is colour coded and the colour scale is shown on the right of each image. Figure 8 shows the cross section of wave propagation speed in the irregularity as a function of the x-coordinate. The dashed line corresponds to the exact solution. Our developed algorithms can be used to reconstruct not only the shape of the irregularity, but also the speed as a function of the coordinate. One can also see that the algorithm reconstructs fairly well even small, 2--5 mm irregularities. Figure 8 clearly shows the ringing effect of the oscillation of the reconstructed image at the locations of the «discontinuity» of the exact solution. These effects are due to the wave nature of ultrasonic sources and, in particular, to the oscillations of the sounding pulse (Fig. 2)

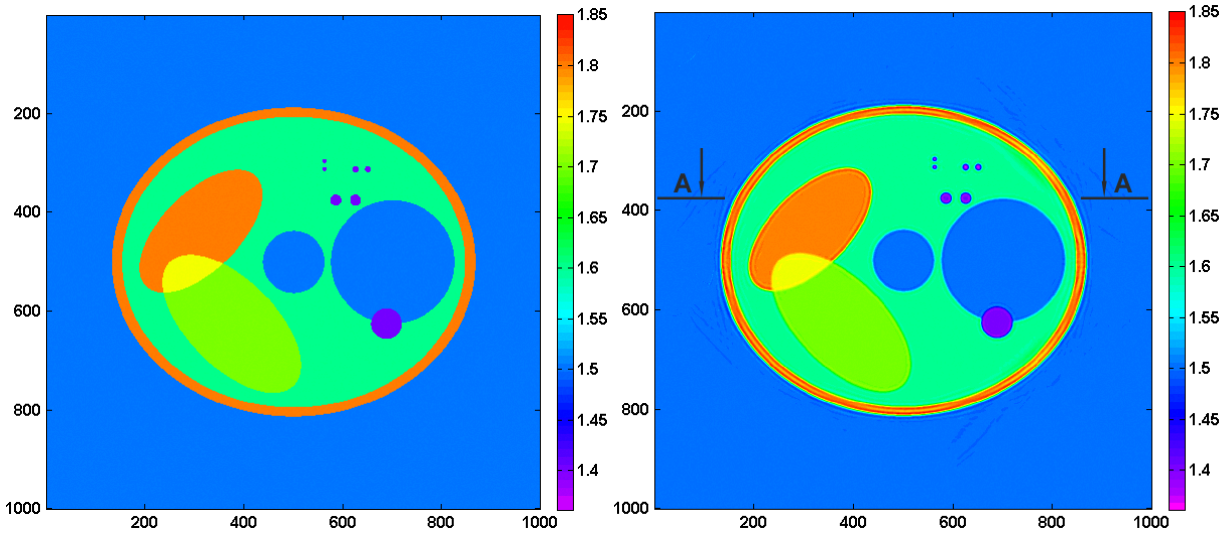

4a **4в**

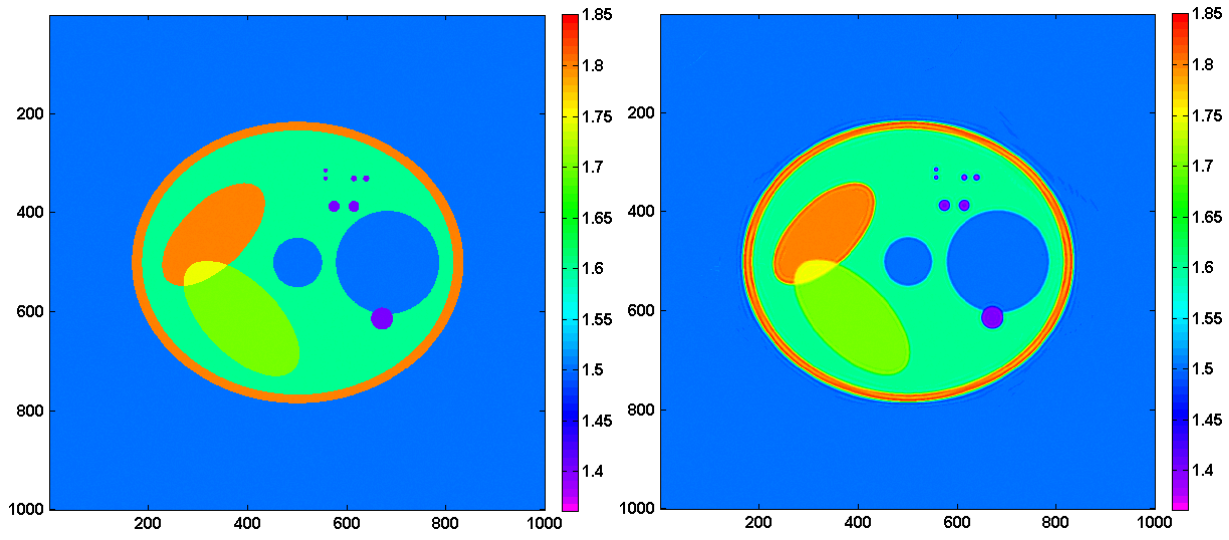

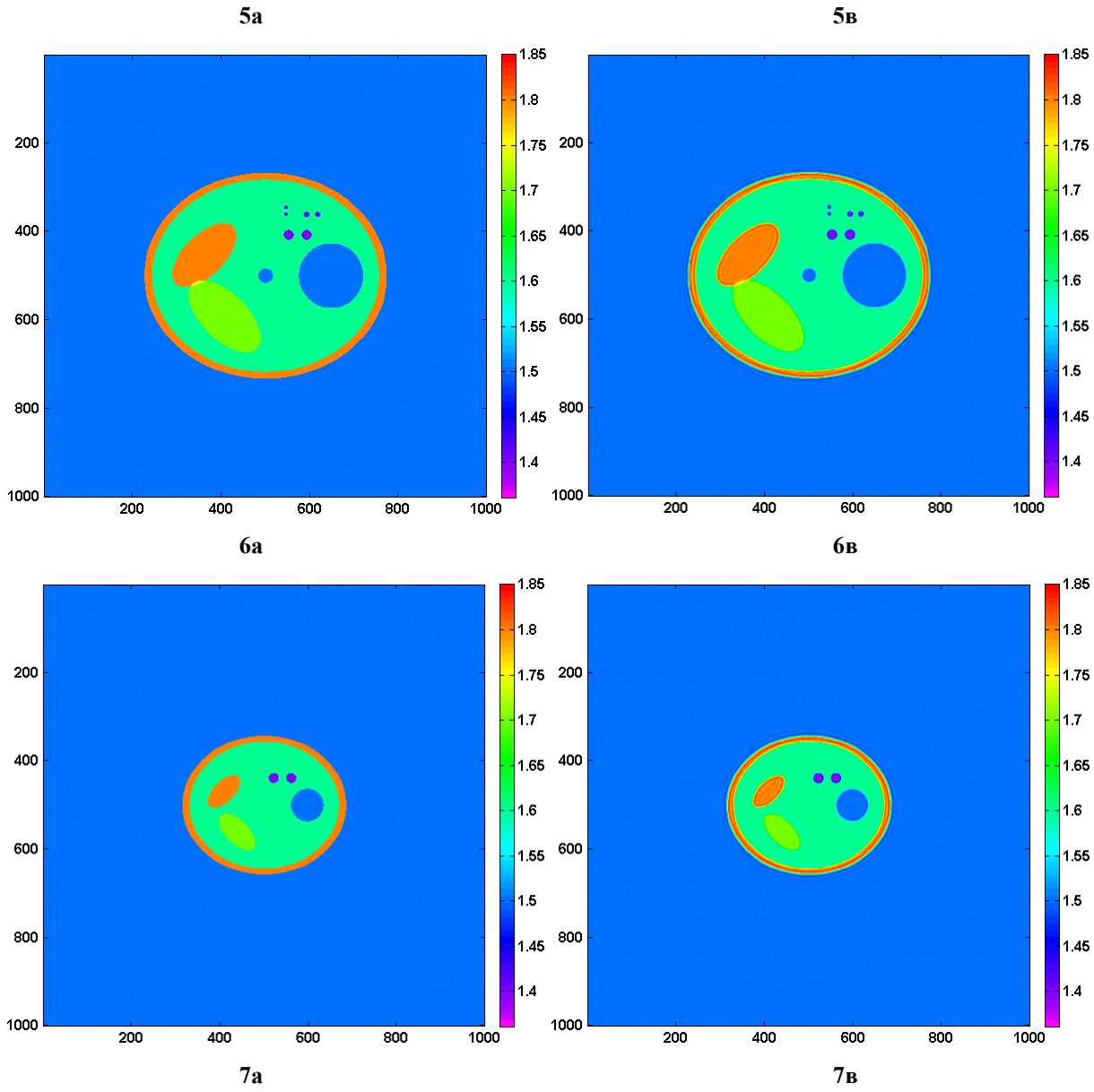

Figure 4-7 (а, в). Model (left panel) and reconstructed (right panel) cross sections of the 3D object.

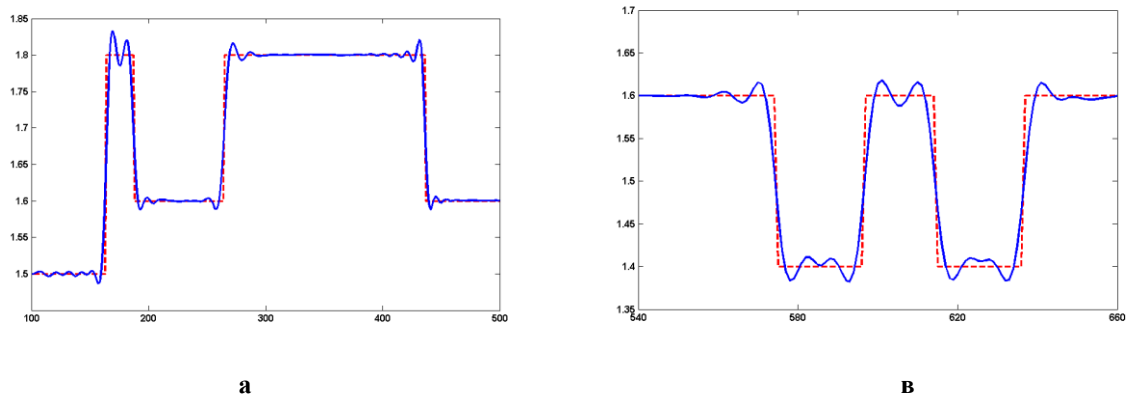

Figure 8a, b. Plots of the cross section along the AA line in Fig. 4b: (a) from pixel 100 to pixel 500 and (b) from pixel 540 to pixel 660

We solved model problems of a fine 1000x1000 grid in *x, y* in a 20x20 cm^2 square and 3000 grid points in *t* in interval from 0 to T. The aim of simulations was to determine the performance limit of ultrasound tomography in the case where the errors were determined by the error of the computation of the direct problem in terms of the adopted model. We chose a fine grid because we used an explicit

difference scheme to solve the direct problem. In these simulations the propagation of the initial pulse in space is approximated on 25 grid points in the coordinates *x* and *y* in order to ensure a good approximation of the Laplacian. It is the need to numerically solve the direct and conjugate problems of wave propagation using explicit schemes that makes it necessary to use a fine grid with about 1000x1000 points. A fine grid in t has to be chosen because of the Courant relation $c^{-0.5}\tau < h$, which ensures the convergence of the explicit scheme.

Reducing the number of grid points in *x*,*y* below 500x500 degrades the quality of the approximation of the differential operators of both the direct and conjugate problems. Simulations show (Figs. 3a--d) that a 500x500 grid in *x*,*y* is quite sufficient for solving problems with several percent errors in initial data.

Let us now consider yet another reason why obtaining very detailed images is a factor of great importance in addressing problems of ultrasonic tomography. Tomographic problems are characterized by two resolutions: the spatial resolution and the resolution in terms of the reconstructed coefficient. This coefficient characterizes density and speed in the case of x-ray and ultrasonic tomography, respectively. The central problem in medicine is how to reveal tumour in the case of small speed deviations that do not exceed 10%. It is very important to determine the shape of the tumour, which to a considerable degree determines whether the tumour is nonmalignant. Rugged (stellate) shape is often indicative of malignant nature of the tumour. To solve the latter task it is important to reconstruct the cross section very precisely.

We now present some of the simulation data that characterize the potential of supercomputers compared to uniprocessor computers.

The steepest descent method ensures monotonic decrease of the residual functional. As is usually the case in minimization problems, the functional of residual first decreases rather rapidly, approaches the error after many iterations, and then practically ceases to decrease. In our model simulations of the inverse problem without introducing extra errors into experimental data we reduced the residual functional by a factor of 10000 after 700 iterations, which took about four hours when run on 20480 CPU cores of "Lomonosov" supercomputer. We obtained this result with the only aim to demonstrate the limiting capabilities of the supercomputer when used to address ultrasonic tomography tasks with very small errors.

When addressing real tasks involving data with errors on the order of several percent the problem can be solved on a 500x500 grid with 300--400 iterations. The use of 2560 CPU cores of the supercomputer makes it possible to solve this problem on 40 layers in ~15 min. This solution reduces the computing time by more than a factor of 1000 compared to uniprocessor computations.

Acoustic wavelength is an important parameter of ultrasonic tomography. The 5 mm wavelength chosen for simulations is greater than the wavelengths usually employed in common ultrasonography. Этот выбор обусловлен тем, что в задачах томографии необходимо получать сигнал на детекторах с высокой точностью. Soft tissues absorb ultrasonic radiation and absorption depends strongly on frequency, or, what is the same, on wavelength. Simulations show that the adopted ~5 mm wavelength range allows cross-section features with sizes smaller than 2 mm to be reconstructed in the case of small errors in initial data. Shorter wavelength, on the one hand, improves the resolution, and, on the other hand, decreases -- because of absorption -- the signal-to-noise ratio. The sounding pulse shown in Fig. 2 actually contains a wide frequency spectrum, which also includes higher frequencies.

6. Conclusion and discussion

1. The aim of this study is to determine the capability limits of ultrasound diagnosis of breast tumour. Inverse problems of ultrasound tomography, even when solved in terms of the simplest wave equation model, reduce to nonlinear coefficient inverse problems. Solving inverse problems on a fine grid to ensure high resolution is impossible without using supercomputers. Our proposed solution algorithms for inverse problems can be used to efficiently solve inverse problems in the above formulation on fine grids with sizes of up to 1000x1000. We thus now have a tool, which can be used to analyze various experimental schemes, the effect on the results of the reconstruction of source and detector properties, wavelength dependence of the results, etc. already at the design stage. As a result, it becomes possible to determine the optimum parameters of tomographic facilities designed.

2. The emphasis in our simulations was on assessing diffraction effects in the solution of inverse problems in terms of the base model (1-3). We show, in terms of the model considered, that cross sections of a three-dimensional object can be, in principle, reconstructed with a high resolution of 2-3 mm or better. These results were obtained in terms of a stationary scheme without elements of rotation (with

fixed transducer positions) in the case of a small number of sources, but sufficiently large number of receivers located ~ $\lambda/2$ apart from each other.

3. Simulations demonstrated that it is possible to reliably reconstruct not only the shape of the irregularity, but also the value of function $c(x,y)$.

4. The most important difficulty of the approximate solution of nonlinear problems is the choice of the initial approximation. Numerous (more than 100) computations of model problems in the domain studied showed that within the parameter domain considered the algorithms developed solve efficiently the inverse problem in iterative schemes starting with the initial approximation $c(x,y)$=const. This may be due to the fact that the speed of sound propagation in human tissue differs from the corresponding speed in both nonmalignant and malignant breast tumour by no more than 10% and hence the adopted initial approximation is close to the global minimum of the functional.

5. Our developed algorithms use the methods of functional minimization well known since the time of Newton -- such as the steepest descent method, which, as shown by simulations, prove to be very efficient for solving the problems of ultrasonic tomography in terms of model (1-3).

6. We wrote out the formula for the gradient of residual in terms of one of the models involving attenuation (5-7), allowing the gradient methods used for inverse problem (1-3) to be applied to the problem with attenuation. In this case two functions - $c(x,y)$ and $a(x,y)$ - are to be reconstructed. The gradient of the functional of residual can be computed by solving the conjugate problem (13-15). The fundamental difference between the conjugate problem (22-24) in terms of model (1-3) and the conjugate problem (13-15) in terms of model (5-7) is that the pulse decays in the model with attenuation in the case of the direct problem. Correspondingly, the wave amplitude $w(r,t)$ increases in the conjugate problem, which is solved backwards in time.

7. The attenuation factor in ultrasonic tomography problems is every bit as important as are diffraction effects. Attenuation really exists and depends strongly on frequency. The signal is totally absorbed at high frequencies > 10 MHz. This wavelength range is used in common ultrasonography facilities to diagnose subcutaneous tissues in the reflective diagnosis mode. Choosing the optimum frequency range for ultrasonic tomography is an important problem. On the one hand, resolution increases with frequency. On the other hand, absorption increases nonlinearly with frequency, resulting in a substantial reduction of the signal-to-noise ratio and, consequently, in the increased error of input data.

Several models have been developed to describe the absorption of ultrasonic radiation. In this paper we propose algorithms for solving the problem in terms of one of the simplest absorption models. We consider assessing the applicability of models, their underlying physical principles, the capabilities of various models to interpret ultrasonic tomography data to be a separate and very demanding task, which lies beyond the scope of this paper.

8. Assessing the possibility of solving the three-dimensional problem of ultrasonic tomography by layers is a separate task of great importance. Standard tomographic scheme of the study of a 3D object by 2D sections is ideal for X-ray tomography. X rays can be absorbed, but they are practically impossible to deflect. The applicability of this approach to ultrasonic tomography is not yet entirely understood. What is the minimum thickness of layers in ultrasonic tomography as a function of frequency for them to be independent of each other? What is quality of reconstruction of a 3D object in the case of multilayer ultrasonic tomography?

Naturally, these problems can and should be addressed experimentally. However, this approach involves a number of difficulties. The point is that real detectors do not ideally coincide with each other, each of them has its three-dimensional power-beam pattern, the initial pulse should be stable and accurately measured, one has to take into account the variation of the signal in the analog part, etc.

There is another approach. We can try to solve the problem via mathematical simulations. The direct problem for a simple 3D object can be solved exactly (preferably analytically) to compute the wave field at the detectors located in a plane. We can then solve the problem of two-dimensional reconstruction of the image and compare the result obtained to the corresponding cross section of the 3D object. As a test body we can use a spherically symmetric 3D object containing a small sphere at its centre. The 2D cross sections can be reconstructed in the case of different spacing between them in order to estimate the distance at which these cross sections become independent of each other. Despite the simple formulation of this problem, its solution involves overcoming a number of difficulties - and some of them are not of computational nature. The computation of the direct and inverse problems should be based on the same mathematical models.

9. Formulas (20) and (21) for the gradient of the functional remain valid both for the two- and three-dimensional case. The proposed supercomputer computational techniques can be formally used to

compute simulated problems for the three-dimensional case, where the domain studied is located inside a three-dimensional cube with the sources and receivers located on its edges. However, solving such problems is a challenging task even for a supercomputer. We believe that this is a difficult, yet undoubtedly solvable task. However, in the case of differential diagnosis of breast cancer of interest are only algorithms that allow irregularities to be reconstructed with a high resolution.

10. The inverse problem with incomplete data, where sources and receivers are located on five edges of the cube with no sources of receivers on the sixth edge, is even more challenging. Such problems -- especially in models with absorption -- cannot be solved without supercomputers.

11. The authors of this paper are ordinary supercomputer users. For us the supercomputer is just an instrument that allows us to solve problems that are beyond the reach of ordinary personal computers. To use a supercomputer, one has not to be an expert in supercomputing technologies. The facility used to obtain the results of this study («Lomonosov») is a general-purpose supercomputer [46]. It has 52000 general-purpose CPU cores, has a peak performance of 1.7 PFlops, and ranks 27th in the TOP500 List. Our programs are based on MPI technology. General-purpose supercomputers are very convenient tools for remote users to develop and debug algorithms and run simulations.

However, the power consumption of such a supercomputer amounts to 2.5 MW, and it is impossible to imagine it as a part of an ultrasonic tomographer. On the other hand, GPU based supercomputers are completely applicable to this end. Such supercomputers having about 40 GPUs can be mounted in one to two "racks" the size of an ordinary refrigerator. The power consumption of a GPU based supercomputer is of about ~20 kW. Such a facility is not too expensive and can be incorporated into an ultrasonic tomographer. Programming GPU based supercomputers is a more difficult task than programming for general-purpose supercomputers, and the algorithms should be custom developed based on the specifics of programming for GPUs.

The seemingly resource hungry explicit schemes of the solution of ordinary differential equations fit ideally the GPU structure, allowing a general-purpose supercomputer to be replaced by two racks with a GPU based supercomputer with a power consumption 20 kW providing a speed gain by a factor of several thousand. Whether a similar result can be achieved using implicit schemes is an open question. This does not mean that the proposed algorithms are optimal from the viewpoint of running on supercomputers. Optimization of numerical algorithms is undoubtedly a task of great importance.

Acknowledgments

We consider to be our pleasant duty to thank Vad.V.Voevodin for his assistance in assessing the efficiency of the operation of algorithms when run on a supercomputer, and to prof. A.B.Bakushinsky for numerous discussions of the work. We are also grateful to acad. V.A.Kubyshkin, the Director of the Vishnevsky Institute of Surgery of the Russian Academy of Medical Sciences, for his advice on medical aspects of the diagnostic of oncological diseases.

This work was supported by the Russian Foundation for Basic Research (project no. 12-07-00304-a).

References

[1] Wiskin J, Borup D T, Johnson S A and Berggren M 2012 Non-linear inverse scattering: High resolution quantitative breast tissue tomography *J. Acoust. Soc. Am.* **131** 3802-13

[2] Duric N et al. 2005 Development of ultrasound tomography for breast imaging: Technical assessment *Medical Physics* **32** 1375–86

[3] Duric N, Littrup P, Poulo L, Babkin A, Pevzner R, Holsapple E, Rama 0 and Glide C 2007 Detection of breast cancer with ultrasound tomography: First results with the Computed Ultrasound Risk Evaluation (CURE) prototype *Medical Physics* **34** 773-85

[4] Gemmeke H, Menshikov A, Tchernikovski D, Berger L, Göbel G, Birk M, Zapf M and Ruiter N V 2010 Hardware setup for the next generation of 3D ultrasound computer tomography *Nuclear Science Symposium Conference Record (NSS/MIC) IEEE* pp 2449-54

[5] Ruiter N V, Schwarzenberg G F, Zapf M, Menshikov A and Gemmeke H 2009 Results of an experimental study for 3D ultrasound CT *NAG/DAGA International Conference on Acoustics* vol 1 pp 305–09

[6] Huang L and Quan Y 2007 Sound-speed tomography using first-arrival transmission ultrasound for a ring array *Medical Imaging 2007: Ultrasonic Imaging and Signal Processing: Proc. SPIE* vol 6513, ed S Y Emelianov and S A McAleavey p 651306
[7] Huang L and Quan Y 2007 Ultrasound pulse-echo imaging using the split-step Fourier propagator *Medical Imaging 2007: Ultrasonic Imaging and Signal Processing: Proc. SPIE* vol 6513, ed S Y Emelianov and S A McAleavey p 651305
[8] Glide C K, Duric N and Littrup P 2007 Novel approach to evaluating breast density utilizing ultrasound tomography *Medical Physics* **34** 744-53
[9] Glide-Hurst C K, Duric N and Littrup P 2008 Volumetric breast density evaluation from ultrasound tomography images *Medical Physics* **35** 3988-97
[10] Jiřík R, Peterlík I, Ruiter N, Fousek J, Dapp R, Zapf M and Jan J 2012 Sound-speed image reconstruction in sparse-aperture 3-D ultrasound transmission tomography *IEEE Transactions on Ultrasonics, Ferroelectrics, and Frequency Control* **59** 254-64
[11] Chavent G 1970 Deux resultats sur le probleme inverse dans les equations aux derivees partielles du deuxieme ordre an t et sur l'unicite de la solution du probleme inverse de la diffusion *Comptes Rendus de l'Académie des Sciences, Series I: Mathematics* **270** 25-8
[12] Lavrent' ev M M, Romanov V G and Shishatskiĭ S P 1986 *Ill-Posed Problems of Mathematical Physics and Analysis* (*Amer. Mathematical Society, Translations of Mathematical Monographs* vol 64)
[13] Ramm A G 1992 *Multidimensional Inverse Scattering Problems* (London: Longman Group)
[14] Colton D and Kress R 1998 *Inverse Acoustic and Electromagnetic Scattering Theory* (Berlin: Springer)
[15] Bakushinsky A B and Goncharsky A V 1994 *Ill-posed Problems. Theory and Applications* (Dordrect: Kluwer Academic Publ.)
[16] Tikhonov A N, Goncharsky A V, Stepanov V V and Yagola A G 1995 *Numerical Methods for the Solution of Ill-Posed Problems* (Dordrecht: Kluwer Academic Publ.)
[17] Yilmaz Ö 2001 *Seismic Data Analysis: Processing, Inversion, and Interpretation of Seismic Data* (*Society of Exploration Geophysicists, Investigations in Geophysics* vol 10)
[18] Schmidt S, Duric N, Li C, Roy O and Huang Z F 2011 Modification of Kirchhoff migration with variable sound speed and attenuation for acoustic imaging of media and application to tomographic imaging of the breast *Medical Physics* **38** 998-1007
[19] Jirik R, Ruiter N, Jan J and Peterlik I 2008 Regularized image reconstruction for ultrasound attenuation transmission tomography *Radioengineering* **2** 125–32
[20] Backushinsky A, Goncharsky A, Romanov S and Seatzu S 1994 On the identification of velocity in seismics and in acoustic sounding *Pubblicazioni dell'istituto di analisa globale e applicazioni, Serie: Problemi non ben posti ed inversi* vol 71 (Florence, Italy: Istituto di Analisi Globale e Applicazioni)
[21] Goncharskii A V and Romanov S Y 2000 On a three-dimensional diagnostics problem in the wave approximation *Computational Mathematics and Mathematical Physics* **40** 1308-11
[22] Natterer F and Wubbeling F 1995 A propagation-backpropagation method for uzltrasound tomography *Inverse Problems* **11** 1225-32
[23] Natterer F 2010 Incomplete data problems in wave equation imaging *Inverse Problems and Imaging* **4** 685-91
[24] Beilina L and Klibanov M V 2012 *Approximate Global Convergence and Adaptivity for Coefficient Inverse Problems* (New York: Springer)
[25] Beilina L and Klibanov M V 2008 A globally convergent numerical method for a coefficient inverse problems *SIAM J.Sci. Comp.* **31** 478-509
[26] Beilina L and Johnson C 2001 Hybrid FEM/FDM method for Inverse scattering problem *Numerical Mathematics and Advanced Applications – ENUMATH 2001* (Springer-Verlag)
[27] Beilina L 2002 Adaptive hybrid FEM/FDM methods for inverse scattering problems *Inverse Problems and Information Technologies* **1** 73-116
[28] Beilina L and Clason C 2006 An adaptive hybrid FEM/FDM method for an inverse scattering problem in scanning acoustic microscopy *SIAM Sci.Comp.* **28** 382-402
[29] Goncharskii A V and Romanov S Y 2012 Two approaches to the solution of coefficient inverse problems for wave equations *Computational Mathematics and Mathematical Physics* **52** 245–51
[30] Goncharskii A V, Ovchinnikov S L and Romanov S Y 2010 On the one problem of wave diagnostic *Moscow University Computational Mathematics and Cybernetics* **34** 1-7
[31] Wiskin J, Borup D T, Johnson S A, Berggren M, Abbott T and Hanover R 2007 Full wave non-linear inverse scattering *Acoustical Imaging* vol 28 ed M Andre (Dordrecht: Springer) pp 183-93
[32] Johnson S A et al. 2005 Breast scanning system *U.S. patent* 7,771,360
[33] Chambers D H, Mast J, Azevedo S G, Wuebbeling F, Natterer F, Duric N, Littrup P J and Holsapple E 2006 Diagnostic analysis of ultrasound data *U.S. patent* 6,984,210
[34] Ashfaq M, Ermert H and Hiltawsky K 2003 Method and holder for spiral computer tomography using ultrasound *EP* 1281354

[35] Dione D P, Staib L H and Smith W 2006 Three-dimensional ultrasound computed tomography imaging system *U.S. patent* 7,025,725
[36] Stotzka R, Kaiser W A and Gemmeke H 2004 Ultrasonic tomograph *U.S. patent* 6,786,868
[37] Johnson S A, Borup D T, Wiskin J W, Natterer F, Wubeling F, Zhang Y and Olsen S C 1999 Apparatus and method for imaging with wavefields using inverse scattering techniques *U.S. patent* 6,005, 916
[38] Bryan T A, Holtz B E, Perleberg G F, Diani F P, Hardie G S and Robertson J C 1997 High-resolution three, dimensional ultrasound imaging device *U.S. patent* 5,673,697
[39] Chang C H, Huang S W, Yang H C, Chou Y H and Li P C 2007 Reconstruction of ultrasonic sound velocity and attenuation coefficient using linear arrays: Clinical assessment *Ultrasound Med. Biol*. **33** 1681–87
[40] Weiwad W, Heinig A, Goetz L, Hartmann H, Lampe D, Buchmann J, Millner R, Spielmann R and Heywang-Koebrunner S H 2000 Direct measurement of sound velocity in various specimens of breast tissue *Invest. Radiol.* **35** 21
[41] Mokhtari-Dizaji M, Vahed M and Gity M 2003 The application of discriminant analysis in differentiation of fibroadenoma and ductal carcinoma of breast tissue using ultrasound velocity measurement *Iran. J. Radiat. Res.* **1** 163
[42] Scherzinger A L, Belgam R A, Carson P L, Meyer C R, Sutherland J V, Bookstein F L and Silver T M 1989 Assessment of ultrasonic computed tomography in symptomatic breast patients by discriminant analysis *Ultrasound Med. Biol.* **15** 21–8
[43] Beilina L, Klibanov M V and Kokurin M Y 2010 Adaptivity with relaxation for ill-posed problems and global convergence for a coefficient inverse problem *J.Mathematical Sciences* **167** 279-325
[44] Natterer F 2008 Acoustic Mammography in the Time Domain *Preprints: Institute of Applied Math. University of Münster*
[45] Engquist B and Majda A 1977 Absorbing boundary conditions for the numerical simulation of waves *Math.Comput.* **31** 629
[46] Voevodin Vl V, Zhumatiy S A, Sobolev S I, Antonov A S, Bryzgalov P A, Nikitenko D A, Stefanov K S and Voevodin Vad V 2012 Practice of "Lomonosov" Supercomputer *Open Systems J.* (Moscow: Open Systems Publ.) **7** http://www.osp.ru/os/2012/07/13017641/ (In Russian)